

Tumor-infiltrating macrophages influence the glycosphingolipid composition of murine brain tumors

Jeffrey A. Ecsedy,* Herbert C. Yohe,^{†,§} Alan J. Bergeron,[†] and Thomas N. Seyfried^{1,*}

Department of Biology,* Boston College, Chestnut Hill, MA, 02167-3811; VA Medical and Regional Office Center,[†] White River Junction, VT, 05009; and Department of Pharmacology,[§] Dartmouth Medical School, Hanover, NH, 03755

Abstract A procedure was developed to analyze glycosphingolipids (GSLs) in tumor-infiltrating macrophages (TIMs). The procedure entailed dissociating tumors into single cell suspensions with a concurrent metabolic labeling of GSLs using [¹⁴C]galactose. TIMs were then separated from tumor cells and other host cells by magnetic activated cell sorting and CD11b (Mac-1) microbeads. Gangliosides and neutral glycosphingolipids were analyzed in the TIM-enriched and TIM-depleted fractions in two different murine brain tumors (EPEN and CT-2A). The TIM gangliosides consisted of over 30 structures as assessed by two-dimensional high performance thin-layer chromatography. GSLs enriched in TIMs, relative to the tumors, included Gg4Cer (asialo GM1), GM1b, and GD1 α . TIM GSLs were similar in EPEN and CT-2A despite their differences in growth and morphology. TIM GSLs were similar whether TIMs were isolated from tumors grown intracranially or subcutaneously. TIM GSLs were also similar to activated peritoneal macrophage GSLs, although differences in the ceramide structure were observed. Knowledge of TIM GSLs will be important in determining the function of these molecules in macrophage-tumor interactions. In addition, these methods will be helpful in determining the cellular origin of human brain tumor GSLs and in identifying tumor-associated GSLs for immunotherapy.—Ecsedy, J. A., H. C. Yohe, A. J. Bergeron, and T. N. Seyfried. **Tumor-infiltrating macrophages influence the glycosphingolipid composition of murine brain tumors.** *J. Lipid Res.* 1998. 39: 2218–2227.

Supplementary key words ganglioside • glycolipid • GM1b • GD1 α • asialo GM1 • macrophage • CD11b • Mac-1 • cancer • astrocytoma • immunotherapy

Brain tumors elicit a response from their host that results in infiltration of macrophages and other host cells into the tumor (1–3). Tumor-associated or tumor-infiltrating macrophages (TIMs) can contribute significantly to the total cell population of some brain tumors (1). We previously suggested that TIMs also contribute to the glycosphingolipid (GSL) composition and to the GSL biosynthetic gene expression of mouse brain tumors (4–7). This hypothesis was based on the observation that the GSL composition and gene expression of mouse brain tumors

grown in culture (in the absence of tumor-infiltrating host cells) were less complex than when grown in vivo (in the presence of tumor-infiltrating host cells).

GSLs are membrane-bound glycoconjugates consisting of a lipophilic ceramide attached to a hydrophilic oligosaccharide chain. The presence of sialic acid on gangliosides distinguishes them from neutral glycosphingolipids (NGSLs). Mouse peritoneal macrophage gangliosides contain two types of sialic acid, N-acetylneuraminic acid (NeuAc) and N-glycolylneuraminic acid (NeuGc) (8, 9). The content and distribution of gangliosides is greater and more complex, respectively, in chemically activated mouse peritoneal macrophages than in resting peritoneal macrophages (8, 9). Resting mouse peritoneal macrophages comprise mostly NeuGc-containing gangliosides (85–90%), whereas activated macrophages contain an even ratio of NeuGc and NeuAc-containing gangliosides (9). Resting mouse peritoneal macrophages contain predominantly GM3–NeuGc, GM1a–NeuGc, and GD1a–NeuGc, whereas activated mouse peritoneal macrophage gangliosides comprise NeuAc and NeuGc-containing GM1a, GM1b, GM2, GD1a, and GD1 α (9–11). The NGSLs of resting and activated mouse peritoneal macrophages comprise GlcCer, LacCer, and Gg4Cer (asialo GM1) as major species (8).

Although immune cell GSLs have been studied extensively, their function in immune mechanisms remains unclear. GSLs may modulate interactions between opposing cells and between cells and the extracellular matrix (12). Such interactions would influence immune cell migration and tissue localization, a function which was attributed to immune cell GSLs (13, 14). GSLs interact with membrane-bound receptors and enzymes in immune cells, therefore they are also implicated as modulators of recep-

Abbreviations: TIM, tumor-infiltrating macrophage; GSL, glycosphingolipid; NGSL, neutral glycosphingolipid; NeuAc, N-acetylneuraminic acid; NeuGc, N-glycolylneuraminic acid; MACS, magnetic activated cell sorting; CD11b[−], CD11b-depleted cell fraction; CD11b⁺, CD11b-enriched cell fraction; MFI F4/80, mean fluorescent intensity of F4/80; HPTLC, high-performance thin-layer chromatography.

¹To whom correspondence should be addressed.

tor mechanisms and signal transduction (15, 16). Activation of immune cells is accompanied by an increase and alteration in GSL expression. It was suggested that changes in immune cell GSL expression correlated with changes in immune cell function (8, 17). This idea was supported by the observation that endotoxin hyporesponsive peritoneal macrophages, which do not undergo normal activation when exposed to stimulating agents, differed in ganglioside content from normal activated peritoneal macrophages (18, 19).

Marked alterations in GSL composition accompany the transformation of normal brain cells into neoplastic tumor cells. These alterations have resulted in a search for tumor-specific or tumor-associated GSLs to be used as targets for tumor diagnosis and therapy (20–22). An analysis of GSLs in tumor-infiltrating host cells, including TIMs, may improve the efficacy of GSL-directed tumor diagnosis and therapy by elucidating the cellular origin of putative tumor-associated GSLs.

In this report, we demonstrate a method for separating TIMs from brain tumors using magnetic activated cell sorting (MACS) and CD11b microbeads for the analysis of GSL composition. In addition, we show that TIMs contribute to the complex GSL composition of brain tumors grown *in vivo*. Preliminary reports of these findings have appeared (23, 24).

MATERIALS AND METHODS

Mice and experimental brain tumors

The C57BL/6J (B6) mice were obtained from The Jackson Laboratory (Bar Harbor, ME) and housed in the Boston College Animal Care Facility using animal husbandry conditions described previously (25). The mice were approximately 2 months of age when used as tumor recipients or for the isolation of peritoneal macrophages. The CT-2A and EPEN experimental mouse brain tumors were maintained by serial transplantations subcutaneously in the flank or in the brain, as described previously (26). Although the exact cell of origin is unknown, both tumors were classified as malignant, poorly differentiated, anaplastic astrocytomas (4). All animal procedures were in strict accordance with the NIH Guide for the Care and Use of Laboratory Animals and were approved by the Institutional Animal Care Committee.

Preparation of mouse peritoneal macrophages

Peritoneal cells were collected from B6 mice as described previously (9). Briefly, peritoneal cells were removed from B6 mice 5 days after intraperitoneal inoculation with 1 ml of 10% thioglycollate (Becton Dickinson). Peritoneal cells were then washed in a hypotonic buffer (0.15 M NH₄Cl, 0.01 M KHCO₃, and 0.1 mM disodium EDTA) to remove contaminating erythrocytes.

Preparation of radiolabeled cells and separation of CD11b⁺ cells

A single-step procedure was used to dissociate tumors and radiolabel GSLs. Intact tumors (approximately 0.5 cm³) or peritoneal cells (approximately 4 × 10⁷) were incubated in 1 ml of RPMI 1640 (Gibco BRL) with 500 μg of type II collagenase (Worthington Biochemical), 0.5 μg deoxyribonuclease type I (Sigma), and 3.0 μCi of [¹⁴C]galactose (52 mCi/mmol, radiolabel on carbon 1, NEN) at 37°C for 4 h on a stir plate. The cells were washed

in PBS/BSA (phosphate-buffered saline, 1% bovine serum albumin, 5 mM EDTA, pH 7.2). The cells were then incubated with CD11b microbeads (20 μl/10⁷ cells, Miltenyi Biotec Inc.) and PBS/BSA (80 μl/10⁷) at 4°C for 25 min. CD11b microbeads comprise an anti-CD11b monoclonal antibody conjugated to a metallic particle. CD11b (also called Mac-1) is highly expressed on the surface of monocytes and macrophages. Unbound microbeads were removed by washing cells with 45 ml of PBS/BSA. The cells were resuspended in PBS/BSA and passed two times over a MACS LS⁺ positive selection column on a MACS separation system (Miltenyi Biotec Inc). CD11b⁻ cells were removed from the columns by washing with 4–5 column volumes of PBS/BSA. The columns were then removed from the MACS separation system and CD11b⁺ cells were eluted by washing with 2–3 column volumes of PBS/BSA.

Analysis of Fc receptor-bearing cells

The erythrocyte/antibody rosette assay was used to estimate the relative proportion of Fc receptor-bearing cells in the dissociated tumor, the CD11b-depleted cell fraction (CD11b⁻ cells), and in the CD11b-enriched cell fraction (CD11b⁺ cells). This assay measures the presence of cell surface IgG Fc receptors that are heavily expressed on macrophages (27). Briefly, 1 × 10⁶ cells from each cell fraction were mixed at room temperature with 1 × 10⁷ sheep erythrocytes that were previously incubated with an anti-sheep erythrocyte antibody (received as a gift from Dr. Robert Evans, The Jackson Laboratory, Bar Harbor, ME). Cells bearing Fc receptors bind the antibody-coated erythrocytes and form rosette-shaped clusters. The rosettes were counted using a hemocytometer.

Flow cytometry

Cells (5 × 10⁵) from each cell fraction were suspended in PBS containing 2% mouse serum (DAKO) and 0.2% BSA. The cell suspensions were then incubated with phycoerythrin (PE)-conjugated F4/80 (received as a gift from Dr. Paul Guyre, Dartmouth Medical School, Lebanon, NH) (5 μl/10⁶ cells) at 4°C for 1 h. F4/80 is a mouse macrophage-specific cell surface antigen. Cells were washed three times using PBS with 0.2% BSA and were fixed in 1% paraformaldehyde in PBS. Flow cytometry was performed using a Becton Dickinson FACScan.

Extraction of total lipids

Extraction of total lipids was performed as previously described (26, 28). Lipids were extracted from samples by adding 5 ml of chloroform–methanol 1:1 (v/v) with 0.5 ml of dH₂O and stirring for 12 h at ambient temperature. Samples were vortexed and then centrifuged for 10 min at 750 g. The supernatant was transferred to another tube and the pellets were washed in 2 ml of chloroform–methanol 1:1 (v/v) and centrifuged for 10 min at 750 g. The resulting supernatant was added to the previous supernatant.

Folch partitioning

Polar and nonpolar lipids from the total lipid extract were separated by Folch partitioning (29). Chloroform (3.5 ml) and water (2.1 ml) were added to the total lipid extracts which were vortexed and centrifuged for 10 min at 750 g. Folch partitioning results in a biphasic system, an upper phase containing polar lipids and a lower phase containing nonpolar lipids. The upper phase was removed and the lower phase was washed with 4.5 ml of chloroform–methanol–water 3:48:47 (v/v/v) by vortexing and centrifuged for 15 min at 750 g. The resulting upper phase was added to the previous upper phase. The lower phase was transferred to another tube and was blown to dryness under a stream of nitrogen.

Ganglioside purification

Gangliosides were purified by modification of previously described methods (26, 28, 30). The combined upper phase from the Folch partition was converted to a chloroform-methanol-water ratio of 30:60:8 (v/v/v) by adding 48 ml of chloroform-methanol 1:2 (v/v). The sample was applied to a diethylaminoethyl (DEAE)-Sephadex A-25 (acetate form) (Pharmacia Biotech) column (1.2 ml bed volume) equilibrated in chloroform-methanol-water 30:60:8 (v/v/v). Non-acidic molecules were eluted from the column with 20 ml of chloroform-methanol-water 30:60:8 (v/v/v). Acidic lipids (gangliosides) were then eluted from the column with 25 ml of chloroform-methanol-0.8 M ammonium acetate ($\text{NH}_4\text{C}_2\text{H}_3\text{O}_2$) 30:60:8 (v/v/v). The solvent was evaporated under vacuum and the gangliosides were base treated in 1 ml of 0.5 N NaOH at 37°C for 1.5 h. Gangliosides were applied to a C18 reverse phase Bond Elute column (Varian) to remove salts and base. The C18 column was initially equilibrated with 5 ml of each of the following: chloroform-methanol 1:1 (v/v), methanol, and 0.1 M NaCl. After applying the gangliosides, the C-18 column was washed with 10 ml of water to remove salts. The gangliosides were eluted from the column with 2 ml of methanol and 4 ml of chloroform. The ganglioside sample was blown to dryness under a stream of nitrogen and resuspended in 0.45 ml of chloroform-methanol-water 30:60:8 (v/v/v). Gangliosides were further purified by applying to a hydroxypropylated dextran (Sephadex LH-20, Pharmacia Biotech) column (9 ml bed volume) equilibrated in chloroform-methanol-water 30:60:8 (v/v/v). Gangliosides were eluted with the same solvent. The first 3-ml fraction represented the void volume and was discarded. The second 3-ml fraction contained the purified gangliosides. The ganglioside sample was blown to dryness under a stream of nitrogen and was resuspended in 1 ml of chloroform-methanol 1:1 (v/v). The procedures used for ganglioside purification result in approximately 90% recovery.

Neutral glycosphingolipid purification

NGSLs were purified by modification of previously described methods (31). Non-polar lipids from the lower phase of the Folch partition were resuspended in 15 ml of chloroform-methanol-water 30:60:8 (v/v/v) and were applied to a DEAE-Sephadex A-25 column prepared as described above. Neutral (non-acidic) lipids were eluted from the column with 20 ml of chloroform-methanol-water 30:60:8 (v/v/v). After evaporating under vacuum, the neutral lipids were base treated in 1 ml of 0.1 N NaOH in methanol at 37°C for 1.5 h. The sample was blown to dryness under a stream of nitrogen and resuspended in 0.45 ml of chloroform-methanol-water 30:60:8 (v/v/v). Base was removed by placing the samples over a Sephadex LH-20 column as described above. The neutral lipids were solubilized in 1 ml of chloroform and were applied to an Iatrobeds silicic acid (Wako Pure Chemicals) column (1.2 ml bed volume). The column was previously equilibrated with 10 ml of each of the following: chloroform-methanol-water 30:60:8 (v/v/v), chloroform-methanol 1:1 (v/v), chloroform-methanol 2:1 (v/v), and chloroform. Free fatty acids, cholesterol, and triglycerides were washed from the column with 30 ml of chloroform and 10 ml of chloroform-methanol 98:2 (v/v). The NGSLs were eluted with 10 ml of each of the following: chloroform-methanol 4:1 (v/v), chloroform-methanol 1:1 (v/v), and chloroform-methanol 1:3 (v/v). The pooled eluate was evaporated and resuspended in 1 ml of chloroform-methanol 1:1 (v/v). The procedures used for NGSL purification result in approximately 90% recovery.

Glycosphingolipid quantitation

The amount of radioactive incorporation into GSLs was estimated by placing a 50- μl aliquot into 6 ml of Ecoscint A (Na-

tional Diagnostits) scintillation solution and counting disintegrations per minute (dpm) on a 1219 Rackbeta Counter (LKB Wallac).

High performance thin-layer chromatography (HPTLC)

Gangliosides were analyzed by two-dimensional HPTLC on Silica Gel 60 plates (E. Merck) as previously described (9). Briefly, gangliosides were spotted 15 mm in and up from the lower left corner of a 10 \times 10 cm HPTLC plate. The plate was chromatographed for 45 min in chloroform-methanol-0.25% aqueous KCl 50:45:10 (v/v/v) and dried with forced air for 15 min and further dried over P_2O_5 for 90 min in a vacuum desiccator. The plate was rotated 90 degrees counter-clockwise and chromatographed in the second dimension in chloroform-methanol-2.5 N aqueous NH_4OH containing 0.25% KCl 50:45:10 (v/v/v) for 30 min and dried as described above. Ganglioside standards (received as gifts from Dr. Robert Yu or obtained from Matreya Inc.) were run on the plate margins in each dimension but are not shown.

NGSLs were analyzed by one-dimensional HPTLC. Briefly, NGSLs were spotted on Silica Gel 60 plates and chromatographed in chloroform-methanol-water 65:35:8 (v/v/v) with 0.02% CaCl_2 for 50 min (31). NGSLs were also spotted on plates pretreated for 30 s with 2.5% $\text{Na}_2\text{B}_4\text{O}_7$ in methanol to separate GlcCer from GalCer (32). The plate was then chromatographed in chloroform-methanol-25% NH_4OH :water 65:35:4:4 (v/v/v/v) until the solvent reached the top of the plate. NGSL standards were received as gifts from Dr. Robert Yu or obtained from Matreya Inc.

Radiolabeled gangliosides and NGSLs were visualized with a Phosphorimager (Molecular Dynamics). Non-radiolabeled GSLs were visualized by spraying plates with resorcinol reagent (gangliosides) or orcinol reagent (NGSLs) and heating at 100°C for 30 min (26, 31).

Thin-layer chromatography immunostaining

Immunostaining for GM1b, GD1 α , and Gg4Cer was performed as previously described (33). Aliquots of gangliosides equivalent to 5 \times 10⁵ cells and 3 \times 10⁶ cells were used for GM1b and GD1 α immunostaining, respectively. NA-6 (mouse anti-GM1b) and KA-17 (mouse anti-GD1 α) monoclonal antibodies were obtained from Dr. Yoshio Hirabayashi, Frontier Research Program, Riken, Japan and diluted 1/500. Peroxidase-conjugated goat anti-mouse IgM secondary antibodies (Jackson ImmunoResearch) were used to visualize gangliosides. An aliquot of NGSLs equivalent to 3 \times 10⁶ cells was used for Gg4Cer immunostaining. Gg4Cer antiserum was obtained from Dr. Robert Yu, Medical College of Virginia, Richmond, VA and diluted 1/40. Peroxidase-conjugated anti-rabbit IgG secondary antibodies (Sigma Immunochemicals) were used to visualize Gg4Cer.

Determination of GM1b, GD1 α , and Gg4Cer distribution

The percent distributions of GM1b and GD1 α in each cell fraction were determined using the Phosphorimager display of the two-dimensional HPTLC plates and Imagequant software (Molecular Dynamics). The absolute pixel values for GM1b, GD1 α , or the total gangliosides were determined using volume integration. Appropriate background values were subtracted from the absolute pixel values to determine the net pixel values. The percent distributions were determined by comparing the net pixel values of GM1b or GD1 α to the net pixel value of the total gangliosides. The percent distribution of Gg4Cer was determined from the one-dimensional HPTLC plates. The net pixel values for Gg4Cer and the total NGSLs were determined by obtaining pixel values above background using area integration. The percent distributions were determined by comparing the net pixel value of Gg4Cer to the net pixel value of the total NGSLs.

RESULTS

The amount of Fc receptor-bearing cells and the mean fluorescent intensity of F4/80 (MFI F4/80) were used to estimate the efficiency of separating TIMs from brain tumors using MACS with CD11b microbeads. The values for the CD11b⁺ cells and the CD11b⁻ cells were normalized to the value for the enzymatically dissociated tumor (total dissociated tumor), which was arbitrarily set to 100% (Fig. 1). TIMs were enriched approximately 400–600% in the CD11b⁺ cells, and were depleted by approximately 50% in the CD11b⁻ cells, as compared to the total EPEN tumor. Our previous findings showed that most thioglycolate-elicited peritoneal cells (mostly macrophages) elute in the CD11b⁺ cell fraction, whereas cultured EPEN and CT-2A tumor cells elute in the CD11b⁻ fraction (23). Taken together, these data indicate that the CD11b⁺ cells comprise mostly TIMs and the CD11b⁻ cells comprise mostly tumor cells and CD11b⁻ host cells.

The rate of ganglioside biosynthesis was similar in the CD11b⁻ and CD11b⁺ cell fractions of the EPEN tumor over the 4-h labeling period (Table 1). In contrast, the rate of ganglioside biosynthesis was significantly lower in the CD11b⁺ cells than in the CD11b⁻ cells of the CT-2A tumor. The rate of NGSL biosynthesis was significantly lower in the CD11b⁺ cells than in the CD11b⁻ cells of both tumors (Table 1). These findings indicate that GSL biosynthesis, in general, was lower in TIMs than in the neoplastic tumor cells.

A schematic identifying gangliosides chromatographed by two-dimensional HPTLC is shown in Fig. 2. These identifications were obtained from previous analyses of mouse macrophage gangliosides (9, 11, 18, 19). The ganglioside distribution of the dissociated EPEN tumor (Total) de-

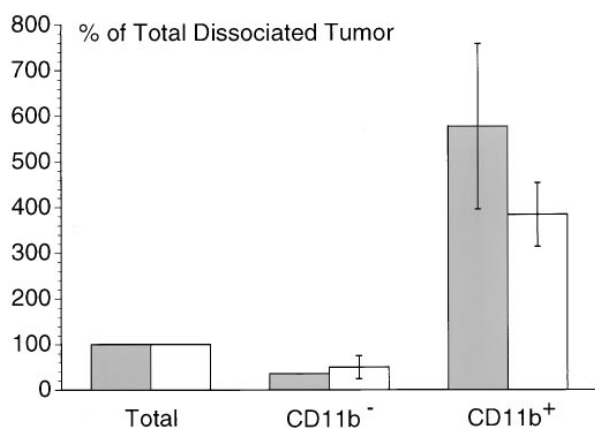


Fig. 1. Relative proportion of Fc receptor-bearing cells (shaded bars) and mean fluorescent intensity of F4/80 (MFI F4/80) (open bars) in the total dissociated tumor (Total); the CD11b-depleted cell fraction (CD11b⁻); and in the CD11b-enriched cell fraction (CD11b⁺). The proportion of Fc receptor-bearing cells and the MFI F4/80 in each cell fraction was normalized to that in the total dissociated tumor which was arbitrarily given the value of 100%. Data were obtained from tumors grown subcutaneously in the flank of B6 mice. Data are mean values from two independent experiments and the range of the two values is shown (bars).

TABLE 1. Rate of GSL biosynthesis in the CD11b⁻ and CD11b⁺ cells isolated from the EPEN and CT-2A tumors

Tumor	Cells Fraction ^a	Ganglioside Biosynthesis	NGSL Biosynthesis
		% of total tumor	
Total EPEN	CD11b ⁻	97 ± 14	100 ± 8
	CD11b ⁺	92 ± 21	67 ± 2 ^b
Total CT-2A	CD11b ⁻	133 ± 6	119 ± 7
	CD11b ⁺	79 ± 11 ^b	67 ± 6 ^b

Rates of ¹⁴C incorporation (dpm) into gangliosides or NGSLS/10⁵ cells/4 h were normalized to that in the total dissociated tumor which was arbitrarily given the value of 100%. Data were obtained from three independent tumors grown subcutaneously in the flank of B6 mice and are expressed as means ± SEM.

^aTotal, total dissociated tumor; CD11b⁻, CD11b-depleted cell fraction; CD11b⁺, CD11b-enriched cell fraction.

^bIndicates that the rate of biosynthesis in the CD11b⁺ fraction is significantly lower than that in the CD11b⁻ fraction ($P < 0.01$, unpaired two-tailed Student's *t* test).

ected by radiolabeling with [¹⁴C]galactose (Fig. 3A) was similar to the distribution in the intact EPEN tumor detected by resorcinol spray (not shown). These findings indicate that the ganglioside pattern of the dissociated tumor after 4 h of radiolabeling was similar to the ganglioside pattern of the solid tumor at the time of resection.

GM3-NeuAc and GM3-NeuGc were the major gangliosides synthesized in the EPEN tumor (Fig. 3A). In addition to these gangliosides, numerous minor ganglioside species were also synthesized. Many of the gangliosides migrated as multiple spots due to heterogeneity in the structure of sialic acids (NeuAc and NeuGc) and ceramide (C16 to C24 fatty acids) (9, 19). The GM3 gangliosides were enriched in the CD11b⁻ cells and were depleted in the CD11b⁺ cells (compare Figs. 3B and 3C). GM3 was the only ganglioside synthesized in the EPEN cultured cells (4). Together, these results show that the EPEN CD11b⁻ cells comprise mostly neoplastic tumor cells.

The ganglioside distribution of the CD11b⁺ cells was extremely complex and consisted of more than 30 distinct structures including GM1a, GM1b, GD1a, and GD1α. GM1b and GD1α are indicated on the HPTLC with arrows and arrow heads, respectively (Fig. 3C). The structures of GM1b and GD1α were corroborated from their positive TLC immunostaining using anti-GM1b and anti-GD1α antibodies, respectively (Fig. 4). Relative to their distribution in the total dissociated tumor, GM1b and GD1α were significantly enriched in the CD11b⁺ cell fraction and were depleted in the CD11b⁻ cell fraction (Fig. 5). Similar results were obtained for the CT-2A tumor. These findings indicate that most of the GM1b and GD1α gangliosides in the EPEN and CT-2A tumors are localized in the TIMs.

Brain tumors are often grown subcutaneously in the flanks of syngeneic mice to avoid contamination from normal CNS tissue that becomes entrapped in intracerebral tumors (26). We found that the overall distribution of gangliosides was similar in EPEN CD11b⁺ cells whether

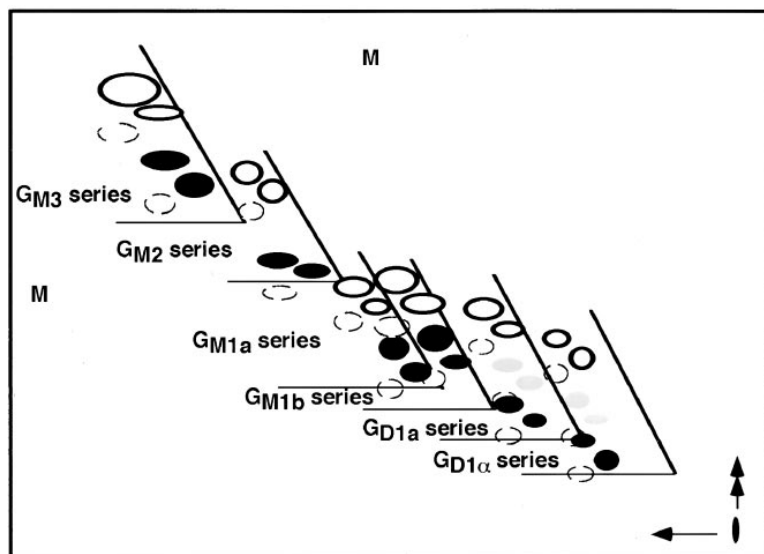


Fig. 2. A schematic used for the localization of gangliosides chromatographed by two-dimensional HPTLC. The schematic represents gangliosides chromatographed in chloroform-methanol-0.25% aqueous KCl 50:45:10 (v/v/v) (first dimension) and chloroform-methanol-2.5 N aqueous NH_4OH containing 0.25% KCl 50:45:10 (v/v/v) (second dimension). The unshaded ellipses indicate NeuAc-containing gangliosides and the darkly filled ellipses indicate NeuGc-containing gangliosides. The shaded ellipses seen in the GD1a and GD1 α series consist of mixed isomers of both sialic acid structures. The broken ellipses indicate the third fatty acid variant of the ceramide in the CD11b⁺ thioglycollate-elicited peritoneal cells. The letter "M" at the top and left side of the schematic indicates the relative mobility of brain GM1a standard.

isolated from tumors grown in the flank or in the brain (compare Figs. 3C and 3D). Similar results were obtained for the CT-2A tumor (data not shown). These findings indicate that different tumor growth environments do not markedly affect the ganglioside composition of TIMs.

Although macrophage number and morphology vary greatly among different types of brain tumors, it is not known to what extent differences in brain tumor type might also influence the ganglioside composition of TIMs. The EPEN tumor is firm, slow growing, and largely avascular, whereas the CT-2A tumor is soft, rapidly growing, and heavily vascularized. The EPEN tumor expresses GM3-NeuAc as the major ganglioside, whereas the CT-2A tumor expresses NeuAc-containing GM3, GM2, GM1a, and GD1a as major gangliosides (4, 5, 26). Despite these differences in growth rate, vascularization, and ganglioside composition, the ganglioside distributions in the CD11b⁺ cells separated from the EPEN and CT-2A tumors were remarkably similar (compare Figs. 3C and 3E). These findings indicate that differences in brain tumor type do not markedly influence the ganglioside composition of TIMs.

Most TIMs are derived from peripheral blood monocytes, but no prior studies have compared the GSL composition of TIMs with that of activated peripheral macrophages. We found that the ganglioside distribution of CD11b⁺ cells from the EPEN and CT-2A tumors was similar to that of peritoneal macrophages elicited with thioglycollate (compare Figs. 3C-E with 3F). Both macrophage populations contained predominantly GM1 and GD1 type gangliosides. However, some differences were observed in the ganglioside distribution. Most of the gangliosides from the CD11b⁺ thioglycollate-elicited peritoneal cells migrated as triplets, whereas most of the gangliosides in the CD11b⁺ cells in both EPEN and CT-2A tumors migrated as doublets. For example, GM3-NeuAc from the peritoneal macrophages appears as three spots in a sideways V formation, whereas GM3-NeuAc from the tumor macrophages appears as two spots. These differences likely reflect differences in the fatty acid composition of the ceramide (19).

The major radiolabeled NGSs in all cell fractions included glucosylceramide (GlcCer), lactosylceramide (LacCer), trihexosylceramide (Gg3Cer), and tetrahexosylceramide (Gg4Cer or asialo GM1) (Fig. 6). As observed for the gangliosides, most of the tumor NGSs migrated as doublets. The two upper bands, migrating at the plate top in all cell fractions, were positively identified as GlcCer using sodium borate-impregnated HPTLC (data not shown). No GalCer was detected in any of the samples. The level of Gg4Cer was noticeably depleted in the CD11b⁻ cells and markedly enriched in the CD11b⁺ cells in both EPEN and CT-2A (Figs. 5 and 6). The structure of Gg4Cer was corroborated by its positive TLC immunostaining using Gg4Cer antiserum (Fig. 4C). No significant differences were seen in the NGS distributions of the CD11b⁺ cells separated from either the EPEN or CT-2A tumors that were grown subcutaneously in the flank or in the brain (data not shown). Gg4Cer was also a major NGS in the activated peritoneal macrophages (Fig. 6). These findings indicate that most of the Gg4Cer in the EPEN and CT-2A tumors is localized in the TIMs.

DISCUSSION

Although macrophages are a major tumor-infiltrating cell of the mouse immune system (27, 34), there have been no prior studies on the GSL composition of TIMs. This has been due largely to the difficulty in separating TIMs from the neoplastic tumor cells and in obtaining enough material for biochemical analysis. We have developed a new method to overcome this problem that entails a one-step dissociation of brain tumors into single cell suspensions with a concurrent metabolic labeling of GSLs using [¹⁴C]galactose. TIMs are then separated from neoplastic tumor cells and other host cells using magnetic activated cell sorting and CD11b microbeads.

Our results showed that TIMs possess an extremely complex ganglioside distribution with more than 30 distinct

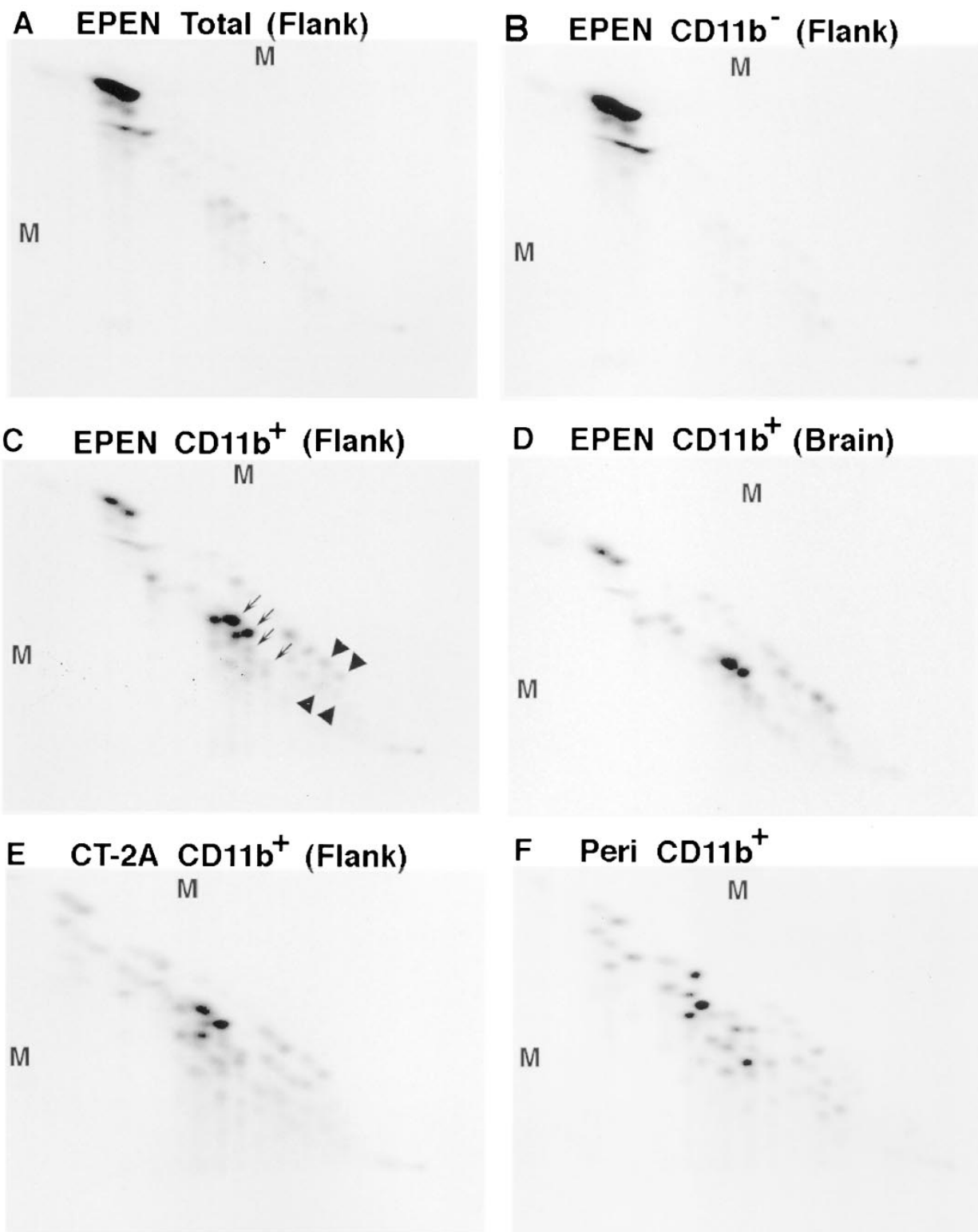


Fig. 3. Two-dimensional high performance thin-layer chromatograms of radiolabeled gangliosides isolated from mouse brain tumors and from macrophage-enriched cell fractions. The tumors were grown either subcutaneously in the flank (Flank) or in the brain (Brain). The peritoneal cells (Peri) were activated with thioglycollate. A: total dissociated EPEN; B: EPEN CD11b-depleted cell fraction; C: EPEN CD11b-enriched cell fraction; D: EPEN CD11b-enriched cell fraction; E: CT-2A CD11b-enriched cell fraction; F: thioglycollate-elicited peritoneal CD11b-enriched cell fraction. Approximately 3000 dpm of ¹⁴C-labeled gangliosides were spotted for each plate. The plates were chromatographed in chloroform-methanol-0.25% aqueous KCl 50:45:10 (v/v/v) (first dimension), chloroform-methanol-2.5 N aqueous NH₄OH containing 0.25% KCl 50:45:10 (v/v/v) (second dimension) and visualized with a Phosphorimager. The arrows in plate C indicate the location of GM1b gangliosides and the arrowheads indicate the location of GD1 α gangliosides. The letter "M" at the top and left side of the images indicates the relative mobility of brain GM1a standard.

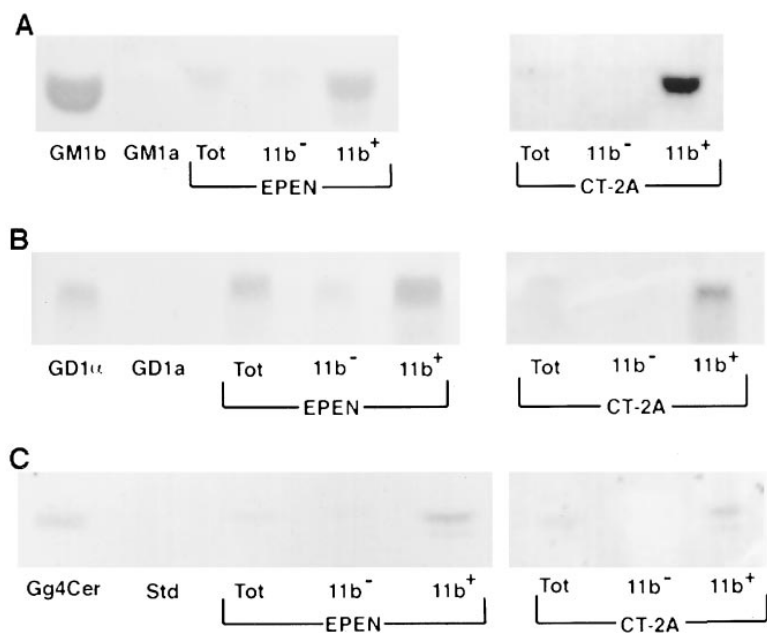


Fig. 4. Thin-layer chromatography immunostaining of the different cell fractions of the EPEN and CT-2A tumors using anti-GM1b antibody (A), anti-GD1 α -antibody (B), or anti-Gg4Cer antibody (C). Total, total dissociated tumor; 11b⁻, CD11b-depleted cell fraction; and 11b⁺, CD11b-enriched fraction. A: Aliquots of ganglioside equivalent to 5×10^5 cells were spotted for each lane. GM1b and GM1a were used as positive and negative controls, respectively. The plates (Nagel Sil G) were developed by one ascending run with chloroform-methanol-water 55:45:10 (v/v/v) containing 0.02% CaCl₂. B: Aliquots of ganglioside equivalent to 3×10^6 cells were spotted for each lane. GD1 α and GD1a were used as positive and negative controls, respectively. The plates were developed as in A. C: Aliquots of NGS equivalent to 3×10^6 cells were spotted for each cell fraction. Gg4Cer and NGS standards (Std, GalCer, LacCer, Gb3Cer, and Gb4Cer) were used as positive and negative controls, respectively. The plates were developed by one ascending run with chloroform-methanol-water 65:35:8 (v/v/v) containing 0.02% CaCl₂. GSLs were obtained from tumors grown subcutaneously in the flank of B6 mice.

structures including GM1a, GM1b, GD1a, and GD1 α . Much of the complexity arose from heterogeneity in sialic acid and ceramide structure. TIM NGSs consisted mostly of GlcCer, LacCer, Gg3Cer, and Gg4Cer. Some GSLs that were enriched in TIMs (GM1b, GD1 α , and Gg4Cer) were present as minor bands in the tumors and were depleted in the neoplastic CD11b⁻ cell fractions, indicating that TIMs contribute to the GSL composition of brain tumors. GM1b, GD1 α , and Gg4Cer are also present on other populations of murine immune cells (35). In addition, the enrichment of Gg4Cer (asialo-GM1) in TIMs is consistent with previous evidence that asialo-GM1 is a major GSL of activated mouse macrophages (6, 8).

In addition to TIMs, other host cells infiltrate brain tumors, including lymphocytes, NK cells, polymorphonuclear granulocytes, and endothelial cells (3, 36–38). These cells contribute less to the GSL composition of EPEN and CT-2A than the TIMs as most of the minor gangliosides in these tumors were enriched in the TIM cell fraction. We also recently suggested that functional T- and B-lymphocytes, which are absent in SCID mice, do not make major contributions to the ganglioside composition of EPEN and CT-2A (39). Large amounts of lymphocytes are present in some brain tumors though (36), and therefore may also contribute to the GSL complexity of tumors.

We have attributed the presence of NeuGc-containing gangliosides in mouse brain tumors grown in vivo to tumor-infiltrating host cells (5–7). This was based on findings that NeuGc-containing gangliosides as well as the expression of genes necessary for NeuGc synthesis were expressed in solid tumors grown in vivo, but disappeared when brain tumor cells were grown in culture in the absence of host cells (5–7). In addition to host cells, it was proposed that neoplastic tumor cells could acquire NeuGc-containing gangliosides directly from the serum and could incorporate NeuGc into their gangliosides in a

cell type specific manner (39, 40). Therefore, the NeuGc sialic acid present in mouse brain tumor gangliosides is derived from both host infiltrating cells and from mouse serum.

We showed that the overall GSL distribution was similar in TIMs and thioglycollate-elicited peritoneal macrophages. The minor differences observed resulted largely from heterogeneity in ceramide fatty acid composition (19). These findings are also consistent with previous observations that the mode of macrophage activation can influence macrophage ganglioside composition (9).

Properties intrinsic to brain tumors influence the degree of TIM infiltration and TIM morphology (41, 42). In this study we found that the GSL composition of TIMs was remarkably similar in the EPEN and CT-2A tumors that differ significantly in growth, morphology, and ganglioside composition. Furthermore, we found that the local environment (brain versus flank) had little effect on the GSL composition of TIMs. The uniformity of TIM GSLs in different environments and in different tumors suggests that the TIM GSLs perform a common function in tumors, e.g., modulating cell-cell or cell-matrix interactions. The TIM-associated gangliosides GM1b and GD1 α —were previously shown to function in endothelial cell adhesion (43). It is possible that these gangliosides modulate the infiltration of macrophages into tumors. This is consistent with previous findings which suggested a role for GSLs in immune cell migration and tissue localization (13, 14).

Gg4Cer is a major GSL in macrophages, lymphocytes, and NK cells (8, 13, 17, 44). Cell surface Gg4Cer was shown to increase in macrophages and T lymphocytes during activation (8, 17). Our results showing the enrichment of Gg4Cer in TIMs are consistent with these findings. Although increased Gg4Cer is a conserved feature of activated immune cells, the function of this molecule remains unclear. Many reports have appeared describing

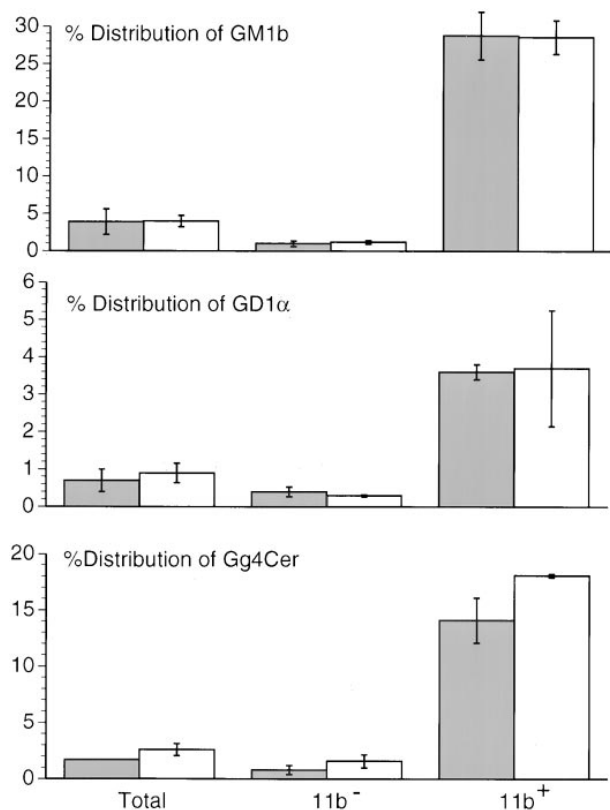


Fig. 5. The percent of the total ganglioside distribution for GM1b and GD1 α , and the percent of the total NGSL distribution for Gg4Cer in the different cell fractions of the EPEN tumor (shaded bars) and the CT-2A tumor (open bars). Total, total dissociated tumor; CD11b⁻, CD11b-depleted cell fraction; and CD11b⁺, CD11b-enriched cell fraction. The percent distribution was determined as described in Materials and Methods. GSLs were obtained from tumors grown subcutaneously in the flank of B6 mice. Data are mean values from two independent experiments and the range of the two values is shown (bars).

immune cell GSLs, but the function of these molecules in tumor immunobiology is unknown. We have provided the first description of GSLs in TIMs. These results can be used for assessing the function of these molecules in macrophage-tumor interactions.

In general, the rate of GSL biosynthesis was less in TIMs than in the neoplastic cells in both the EPEN and CT-2A tumors. Because TIMs are mostly non-dividing cells while the neoplastic cells divide rapidly, the differences in GSL biosynthesis likely reflect differences in cell proliferation. Similarly, the higher relative rate of GSL biosynthesis in the CT-2A neoplastic cells (CD11b⁻ fraction) than in the EPEN neoplastic cells likely reflects the faster growth rate of the CT-2A tumor over the EPEN tumor. However, the higher GSL biosynthesis rate in neoplastic cells over TIMs is not associated with a higher content of GSLs. This notion comes from previous findings that ganglioside content is significantly higher in activated macrophages than in the EPEN or CT-2A tumor cells (4, 9, 45). This discrepancy between rate of biosynthesis and absolute amount of gangliosides in the TIM and neoplastic cell fractions may

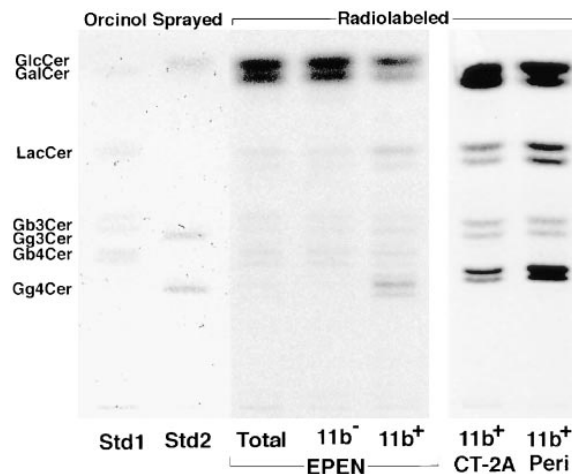



Fig. 6. High performance thin-layer chromatogram of radiolabeled NGSLs isolated from mouse brain tumors and from macrophage-enriched cell fractions. The tumors were grown subcutaneously in the flank of B6 mice. The peritoneal cells (Peri) were activated with thioglycollate. Std1, GalCer, LacCer, Gb3Cer, and Gb4Cer; Std2, GlcCer, Gg3Cer, and Gg4Cer; Total, total dissociated tumor; 11b⁻, CD11b-depleted cell fraction; 11b⁺, CD11b-enriched cell fraction. Approximately 2000 dpm of ¹⁴C-labeled NGSLs were spotted for the radiolabeled lanes. The plates were developed by one ascending run with chloroform-methanol-water 65:35:8 (v/v/v) containing 0.02% CaCl₂. After visualizing radiolabeled lanes with a Phosphorimager, the plates were sprayed with the orcinol reagent and heated to 100°C to visualize the standards.

reflect differences in ganglioside turnover which is likely lower in TIMs than in neoplastic tumor cells. Hence, relatively few TIMs may contribute significantly to the GSL composition of brain tumors.

GSLs may be useful targets for tumor therapy because they are present on the cell surface, are structurally diverse, and vary significantly in composition between normal brain and brain tumors. The potential of antigen-directed immunotherapy has not been fully realized due to several problems. Most monoclonal approaches have been ineffective due to the antigenic heterogeneity of tumors, the inability to stimulate the patients own effector mechanisms, insufficient cytotoxicity, and the rapid elimination of antibodies from the circulation (46-49). Cross-reactivity with normal host cells is another significant problem with monoclonal immunotherapy. Our method for the analysis of GSLs in TIMs could be used for other infiltrating host cells and therefore should be useful for accurately defining the cellular origin of putative tumor-associated GSLs.

Our findings provide the first direct evidence that macrophages contribute to the GSL complexity of mouse brain tumors. Furthermore, the GSL composition of TIMs was similar to that of activated peritoneal macrophages. As macrophages can comprise up to 78% of the cell population in some human brain tumors (1), it is probable that TIMs also influence the GSL composition of human brain tumors. In addition to brain tumors, TIMs likely influence the GSL composition of other forms of cancer. The association of tumorigenesis with alterations in GSLs has led to

the search for tumor-specific or tumor-associated GSLs for use in tumor diagnosis and therapy. Our results indicate that many tumor-associated GSLs can be enriched in tumor-infiltrating host cells. Hence, the use of GSLs for tumor diagnosis and therapy may be improved with knowledge of their cellular location. 

We thank Dr. Robert Evans, Dr. Paul Guyre, Dr. Yoshio Hirobayashi, and Dr. Robert Yu for the generous gifts of antibodies. We also thank Dr. John Brigande, Mark Manfredi, and Mary Griffith for technical assistance and helpful discussions. This work was supported by an NIH RO1 Grant (NSCA33640), the Boston College Research Expense Fund, and a Veterans Administration Merit Review (to H. C. Y).

Manuscript received 29 May 1998 and in revised form 24 July 1998.

REFERENCES

- Wood, G. W., and R. A. Morantz. 1979. Immunohistologic evaluation of the lymphoreticular infiltrate of human central nervous system tumors. *J. Natl. Cancer Inst.* **62**: 485–491.
- Rossi, M. L., J. T. Hughes, M. M. Esiri, H. B. Coakham, and D. B. Brownell. 1987. Immunohistological study of mononuclear cell infiltrate in malignant gliomas. *Acta Neuropathol. Berl.* **74**: 269–277.
- Leenstra, S., D. Troost, P. K. Das, N. Claessenk, A. E. Becker, and A. Bosch. 1993. Endothelial cell marker PAL-E reactivity in brain tumor, developing brain, and brain disease. *Cancer*. **72**: 3061–3067.
- Seyfried, T. N., M. El-Abbadi, and M. L. Roy. 1992. Ganglioside distribution in murine neural tumors. *Mol. Chem. Neuropathol.* **17**: 147–167.
- El-Abbadi, M., and T. N. Seyfried. 1994. Influence of growth environment on the ganglioside composition of an experimental mouse brain tumor. *Mol. Chem. Neuropathol.* **21**: 273–285.
- Seyfried, T. N., M. El-Abbadi, J. A. Ecsedy, H. W. Bai, and H. C. Yohe. 1996. Influence of host cell infiltration on the glycolipid content of mouse brain tumors. *J. Neurochem.* **66**: 2026–2033.
- Ecsedy, J. A., M. G. Manfredi, H. C. Yohe, and T. N. Seyfried. 1997. Ganglioside biosynthetic gene expression in experimental mouse brain tumors. *Cancer Res.* **57**: 1580–1583.
- Mercurio, A. M., G. A. Schwarting, and P. W. Robbins. 1984. Glycolipids of the mouse peritoneal macrophage. Alterations in amount and surface exposure of specific glycolipid species occur in response to inflammation and tumoricidal activation. *J. Exp. Med.* **160**: 1114–1125.
- Yohe, H. C., D. L. Coleman, and J. L. Ryan. 1985. Ganglioside alterations in stimulated murine macrophages. *Biochim. Biophys. Acta.* **818**: 81–86.
- Yohe, H. C., Y. Song, B. B. Reinhold, and V. N. Reinhold. 1997. Structural characterization of the disialoganglioside of murine peritoneal macrophages. *Glycobiology.* **4**: 1215–1227.
- Macala, L. J., and H. C. Yohe. 1995. In situ accessibility of murine macrophage gangliosides. *Glycobiology.* **5**: 67–75.
- Fishman, P. H. 1986. Recent advances in identifying the functions of gangliosides. *Chem. Phys. Lipids.* **42**: 137–151.
- Muthing, J., H. Egge, B. Kniep, and P. F. Muhlrardt. 1987. Structural characterization of gangliosides from murine T lymphocytes. *Eur. J. Biochem.* **163**: 407–416.
- Berenson, C. S., M. A. Patterson, M. A. Pattoli, and T. F. Murphy. 1996. A monoclonal antibody to human macrophage gangliosides inhibits macrophage migration. *J. Leukocyte Biol.* **59**: 371–379.
- Morrison, W. J., K. Young, H. Offner, and A. A. Vandenberg. 1993. Ganglioside (GM1) distinguishes the effects of CD4 on signal transduction through the TCR/CD3 complex in human lymphocytes. *Cell. Mol. Biol. Res.* **39**: 159–165.
- Yates, A. J., and A. Rampersaud. 1998. Sphingolipids as receptor modulators. *Ann. NY Acad. Sci.* **845**: 57–72.
- Stout, R. D., G. A. Schwarting, and J. Suttles. 1987. Evidence that expression of asialo-GM1 may be associated with cell activation. Correlation of asialo-GM1 expression with increased total cellular

- RNA and protein content in normal thymocyte and spleen cell populations. *J. Immunol.* **139**: 2123–2129.
- Yohe, H. C., and J. L. Ryan. 1986. Ganglioside expression in macrophages from endotoxin responder and nonresponder mice. *J. Immunol.* **137**: 3921–3927.
- Yohe, H. C., C. L. Cuny, L. J. Macala, M. Saito, W. J. McMurray, and J. L. Ryan. 1991. The presence of sialidase-sensitive sialosyl-gangliotetraosyl ceramide (GM1b) in stimulated murine macrophages. Deficiency of GM1b in *Escherichia coli*-activated macrophages from the C3H/HeJ mouse. *J. Immunol.* **146**: 1900–1908.
- Hakomori, S. 1985. Aberrant glycosylation in cancer cell membranes as focused on glycolipids: overview and perspectives. *Cancer Res.* **45**: 2405–2414.
- Wikstrand, C. J., D. C. Longee, R. E. McLendon, G. N. Fuller, H. S. Friedman, P. Fredman, L. Svennerholm, and D. D. Bigner. 1993. Lactotetraose series ganglioside 3',6'-isoLD1 in tumors of central nervous and other systems in vitro and in vivo. *Cancer Res.* **53**: 120–126.
- Sung, C. C., D. K. Pearl, S. W. Coons, B. W. Scheithauer, P. C. Johnson, and A. J. Yates. 1994. Gangliosides as diagnostic markers of human astrocytomas and primitive neuroectodermal tumors. *Cancer*. **74**: 3010–3022.
- Ecsedy, J. A., H. C. Yohe, and T. N. Seyfried. 1997. Glycosphingolipid composition of tumor-infiltrating macrophages isolated from murine brain tumors. *J. Neurochem.* **66** (Suppl.): S12 (Abstract).
- Ecsedy, J. A., H. C. Yohe, A. J. Bergeron, and T. N. Seyfried. 1998. Glycosphingolipid composition of tumor-infiltrating macrophages in brain tumors. *Proc. Am. Assoc. Cancer Res.* **39**: 211.
- Flavin, H. J., A. Wieraszko, and T. N. Seyfried. 1991. Enhanced aspartate release from hippocampal slices of epileptic (EL) mice. *J. Neurochem.* **56**: 1007–1011.
- Seyfried, T. N., R. K. Yu, M. Saito, and M. Albert. 1987. Ganglioside composition of an experimental mouse brain tumor. *Cancer Res.* **47**: 3538–3542.
- Evans, R. 1977. Effect of X-irradiation on host-cell infiltration and growth of a murine fibrosarcoma. *Br. J. Cancer.* **35**: 557–566.
- Seyfried, T. N., G. H. Glaser, and R. K. Yu. 1978. Cerebral, cerebellar, and brain stem gangliosides in mice susceptible to audiogenic seizures. *J. Neurochem.* **31**: 21–27.
- Folch, J., M. Lees, and G. H. Sloane Stanley. 1957. A simple method for the isolation and purification of total lipides from animal tissues. *J. Biol. Chem.* **226**: 497–509.
- Brigande, J. V., F. M. Platt, and T. N. Seyfried. 1998. Inhibition of glycosphingolipid biosynthesis does not impair growth or morphogenesis of the postimplantation mouse embryo. *J. Neurochem.* **70**: 871–882.
- Seyfried, T. N., and T. Ariga. 1992. Neutral glycolipid abnormalities in a t-complex mutant mouse embryo. *Biochem. Genet.* **30**: 557–565.
- Kean, E. L. 1996. Separation of gluco- and galactocerebrosides by means of borate thin-layer chromatography. *J. Lipid Res.* **7**: 449–452.
- Saito, M., N. Kasai, and R. K. Yu. 1985. In situ immunological determination of basic carbohydrate structures of gangliosides on thin-layer plates. *Anal. Biochem.* **148**: 54–58.
- Evans, R., and E. M. Lawler. 1980a. Macrophage content and immunogenicity of C57BL/6J and BALB/cByJ methylcholanthrene-induced sarcomas. *Int. J. Cancer.* **26**: 831–835.
- Muthing, J., B. Schwinzer, J. Peter-Katalinic, H. Egge, and P. F. Muhlrardt. 1989. Gangliosides of murine T lymphocyte subpopulations. *Biochemistry.* **28**: 2923–2929.
- Safdari, H., F. H. Hochberg, and E. Richardson, Jr. 1985. Prognostic value of round cell (lymphocyte) infiltration in malignant gliomas. *Surg. Neurol.* **23**: 221–226.
- Rossi, M. L., N. R. Jones, E. Candy, J. A. Nicoll, J. S. Compton, J. T. Hughes, M. M. Esiri, T. H. Moss, F. F. Cruz-Sanchez, and H. B. Coakham. 1989. The mononuclear cell infiltrate compared with survival in high-grade astrocytomas. *Acta Neuropathol. Berl.* **78**: 189–193.
- Arosarena, O., C. Guerin, H. Brem, and J. Laterra. 1994. Endothelial differentiation in intracerebral and subcutaneous experimental gliomas. *Brain Res.* **640**: 98–104.
- Seyfried, T. N., M. El-Abbadi, J. A. Ecsedy, and H. C. Yohe. 1998. Ganglioside composition of a mouse brain tumor grown in the severe combined immunodeficiency (SCID) mouse. *Mol. Chem. Neuropathol.* **33**: 27–37.
- Kawashima, I., H. Ozawa, M. Kotani, M. Suzuki, T. Kawano, M. Gombuchi, and T. Tai. 1993. Characterization of ganglioside expres-

- sion in human melanoma cells: immunological and biochemical analysis. *J. Biochem. Tokyo*. **114**: 186–193.
41. Schackert, G., R. D. Simmons, T. M. Buzbee, D. A. Hume, and I. J. Fidler. 1988. Macrophage infiltration into experimental brain metastases: occurrence through an intact blood–brain barrier. *J. Natl. Cancer Inst.* **80**: 1027–1034.
 42. Leek, R. D., C. E. Lewis, R. Whitehouse, M. Greenall, J. Clarke, and A. L. Harris. 1996. Association of macrophage infiltration with angiogenesis and prognosis in invasive breast carcinoma. *Cancer Res.* **56**: 4625–4629.
 43. Taki, T., D. Ishikawa, M. Ogura, M. Nakajima, and S. Handa. 1997. Ganglioside GD1alpha functions in the adhesion of metastatic tumor cells to endothelial cells of the target tissue. *Cancer Res.* **57**: 1882–1888.
 44. Kasai, M., M. Iwamori, Y. Nagai, K. Okumura, and T. Tada. 1980. A glycolipid on the surface of mouse natural killer cells. *Eur. J. Immunol.* **10**: 175–180.
 45. Seyfried, T. N., A. M. Novikov, R. A. Irvine, and J. V. Brigande. 1994. Ganglioside biosynthesis in mouse embryos: sialyltransferase IV and the asialo pathway. *J. Lipid Res.* **35**: 993–1001.
 46. Khazaeli, M. B., R. M. Conry, and A. F. LoBuglio. 1994. Human immune response to monoclonal antibodies. *J. Immunother.* **15**: 42–52.
 47. Kurpad, S. N., C. J. Wikstrand, and D. D. Bigner. 1994. Immunobiology of malignant astrocytomas. *Semin. Oncol.* **21**: 149–161.
 48. Uttenreuther-Fischer, M. M., C. S. Huang, and A. L. Yu. 1995. Pharmacokinetics of human–mouse chimeric anti-GD2 mAb ch14.18 in a phase I trial in neuroblastoma patients. *Cancer Immunol. Immunother.* **41**: 331–338.
 49. Pancook, J. D., J. C. Becker, S. D. Gillies, and R. A. Reisfeld. 1996. Eradication of established hepatic human neuroblastoma metastases in mice with severe combined immunodeficiency by antibody-targeted interleukin-2. *Cancer Immunol. Immunother.* **42**: 88–92.